The International Archives of the Photogrammetry, Remote Sensing and Spatial Information Sciences, Volume XLIX-B3-2026
XXV ISPRS Congress 2026 "From Imagery to Understanding", Commission III, 4–11 July 2026, Toronto, Canada

Quality Control For Large-Scale Bundle Adjustment Of Planetary Remote Sensing Images

Xun Geng[1,2], Pengying Liu[1,2], Honghai Ma[1], Jia Wang[3], Zhen Peng[1,2], Jin Wang[1,2,*], Yuying Wang[1,2], Yinhui Wang[1,2], Jianwei Xu[1,2], Guohua Chang[1,2], Can Feng[1,2]

[1] State Key Laboratory of Spatial Datum, Henan University, Zhengzhou, China, 450046
[2] College of Geographic Sciences, Henan University, Zhengzhou, China, 450046
[3] Beijing Aerospace Flight Control Center, Beijing, China, 100094
gengxun@henu.edu.cn (X. Geng), wangjin@henu.edu.cn (J. Wang)

Keywords: Bundle Adjustment, Control Network, Planetary Photogrammetry, Lunar Mapping, Quality Control

Abstract

High-accuracy planetary mapping products are increasingly required for landing-site assessment, precision navigation, and future surface operations on the Moon and Mars. Although massive orbital remote sensing images are available, the geometric accuracy and spatial resolution of many existing mapping products is still insufficient for engineering applications. A major bottleneck is large-scale bundle adjustment, whose reliability is strongly affected by data quality, control network strength, as well as engineering experience. Compared with Earth observation photogrammetry, planetary mapping faces great challenges such as heterogeneous sensor models, complex illumination, sparse absolute control. This paper summarizes a practical quality control framework for large-scale bundle adjustment of planetary remote sensing images. The workflow is divided into four coupled stages: data preprocessing, control network construction, parameter setting, and accuracy evaluation. The framework is distilled from previous planetary mapping studies, open-source software platforms and our practical experience in processing tens of thousands of planetary images. Experiments using LRO NAC datasets demonstrate that satisfactory bundle adjustment results can be achieved when the proposed strategy is applied. The framework improves the overall efficiency, controllability, and reliability of large-scale planetary photogrammetric processing.

1. Introduction

High-precision mapping products are a basic requirement for future planetary exploration. Safe landing, surface traverse planning, and long-term operation on the Moon and Mars rely heavily on large-scale planetary maps. Although planetary image resources are already abundant, many existing mapping products still suffer from limited geometric accuracy and spatial resolution. For example, the Lunar Reconnaissance Orbiter (LRO) Narrow-Angle Camera (NAC) has acquired more than two million images of the lunar surface with spatial resolution of 0.8–1.5 meters (Robinson et al., 2010), and the Mars Reconnaissance Orbiter Context Camera (MRO CTX) and the Mars Express High Resolution Stereo Camera (MEX HRSC) enable the acquisition of near-global or global Martian imagery with spatial resolutions ranging from meters to decameters. However, the grid spacing of global lunar Digital Elevation Models (DEMs) remains on the order of tens of meters, whereas Martian DEMs are on the order of hundreds of meters. One major reason is that large-scale bundle adjustment remains a bottleneck in high-accuracy planetary mapping. Although its mathematical foundation is similar to that in terrestrial photogrammetry, planetary mapping is harder in practice because images are acquired over long time spans, under highly variable illumination, and with sparse or uneven absolute control. Representative studies have shown that large-scale bundle adjustment should be treated as a complete engineering workflow rather than a purely algorithm optimization step. Controlled Mars CTX mosaics and recent lunar south-polar studies both indicate that quality control is central to reliable planetary bundle adjustment (Robbins et al., 2020, Robbins et al., 2023, Chen et al., 2024).

The growing use of artificial intelligence and deep learning in photogrammetry does not eliminate the need for quality control. Improved image matching ability can improve some steps such as automatic tie points extraction, but it cannot compensate for unsuitable image selection, weak control network strength, or unreasonable parameter settings. In this paper, we summarize such a framework for large-scale bundle adjustment of planetary remote sensing images. Rather than introducing a single new optimized bundle adjustment algorithm, we organize experiences from previous planetary mapping studies, common software platforms such as U.S. Geological Survey (USGS) Integrated Software for Imagers and Spectrometers (ISIS) and National Aeronautics and Space Administration (NASA) Ames Stereo Pipeline (ASP), and our own processing of massive lunar and Martian images into a reusable workflow. The framework consists of four interconnected stages: data preprocessing, control network construction, parameter setting during bundle adjustment, and post-adjustment accuracy evaluation. Although the discussion is mainly based on traditional photogrammetric processing, the framework is also applicable to modern learning-based pipelines.

2. Related Work

2.1 General Progress in Large-Scale Bundle Adjustment

Bundle adjustment is one of the core procedures in photogrammetry and directly determines the quality of derived products such as Digital Orthophoto Maps (DOMs) and DEMs. In terrestrial and satellite photogrammetry, large-scale block adjustment has been studied extensively. Li et al. (Li et al., 2023) reviewed

* Corresponding author

the development of large-scale block adjustment from satellite to indoor photogrammetry and pointed out that image matching, model formulation, parameter estimation, and gross-error detection remain the key components of large-scale workflows. Their review also emphasized that the integration of AI, high-performance computing, and big-data technologies is reshaping photogrammetry, but does not remove the need for robust quality control. Yang et al. (Yang et al., 2017) and Pi et al. (Pi et al., 2022) showed that large-scale adjustment depends not only on estimation theory, but also on robust mismatch elimination, and rational constraint. These insights are relevant to planetary mapping, but practical planetary projects still require dedicated quality-control strategies adapted to planetary data characteristics.

2.2 Planetary Bundle Adjustment and Software Platforms

Planetary photogrammetry has benefited greatly from open-source platforms such as USGS ISIS and NASA ASP. In particular, USGS ISIS provides powerful bundle adjustment software tools (e.g., JIGSAW) for extraterrestrial photogrammetry (Edmundson et al., 2012), whereas ASP provides an open-source and widely adopted processing environment for stereo reconstruction (Beyer et al., 2018). These software tools have become standard infrastructure for many planetary mapping projects. Nevertheless, photogrammetric software platforms alone do not guarantee reliable mapping products for large-scale planetary photogrammetric projects.

Another important difference from Earth observation photogrammetry lies in the choice of geometric model. For many terrestrial satellite products, rational polynomial coefficient (RPC) is adopted because orbit and attitude determination can already provide relatively stable sensor geometry, and the RPC parameters offers good software generality for downstream photogrammetric processing. But in planetary mapping, absolute navigation accuracy is often weaker and sensor models are more heterogeneous (Geng et al., 2020). As a result, rigorous sensor models are still the mainstream basis for high-accuracy planetary bundle adjustment. Accordingly, the present study mainly discusses rigorous geometric modeling for push-broom planetary images.

At the same time, current planetary software platforms still have important limitations for very-large-scale projects. First, control-network construction remains a major bottleneck. Existing ISIS workflows are powerful but still rely heavily on careful overlap analysis, matching strategy design, and iterative outlier removal. Second, although ISIS provides rich functionality and detailed bundle adjustment reports, its overall level of automation is still lower than that of mainstream Structure from Motion (SfM) pipelines such as Agisoft Metashape (formerly known as PhotoScan). Thus, successful processing depends strongly on engineering experience. Third, the control network data structures and editing-oriented workflows in USGS ISIS are helpful for quality inspection, but they can also become cumbersome when millions of measures must be organized and refined. Finally, software interoperability in planetary photogrammetry remains limited. Part of the USGS ISIS processing chain can be parsed by NASA ASP, and some datasets (e.g., LRO NAC) can be exported to SOCET SET (developed by BAE Systems) after model conversion. However, planetary data processing still faces broader obstacles related to format compatibility, the scarcity of ground control, coordinate-reference conventions, and the limited support for rigorous sensor models in general-purpose photogrammetric software. These limitations help explain why large-scale planetary bundle adjustment still requires an explicit quality-control framework.

2.3 Controlled Mapping of Extraterrestrial Bodies

A number of studies have demonstrated the feasibility and necessity of large-scale controlled mapping for the Moon and Mars. Wu et al. (Wu et al., 2014), Di et al. (Di et al., 2017), Li et al. (Li et al., 2018), and Ren et al. (Ren et al., 2019) showed that integrated control and external elevation constraints are indispensable when generating lunar mapping products from massive lunar remote sensing images. Recent lunar south-polar mapping studies further emphasize the role of quality control in difficult terrain and complex illumination conditions, especially the need for DEM-based constraints, robust outlier elimination, and suitable function model (Chen et al., 2024, Liu et al., 2024). Controlled mosaicking based on MRO CTX images provides particularly informative examples of large-scale adjustment practice. Robbins et al. (Robbins et al., 2020, Robbins et al., 2023) and Geng et al. (Geng et al., 2022) showed that the quality and reliability of control network are essential to large-scale controlled Mars mapping. Related HRSC, THEMIS, and Mercury studies complement this (Sidiropoulos et al., 2018, Putri et al., 2019, Fergason et al., 2013, Preusker et al., 2017). For difficult lunar polar images, Wang et al. (Wang et al., 2025) demonstrated that control network construction can be strengthened by matching LRO NAC approximate orthophotos with shaded Lunar Orbiter Laser Altimeter (LOLA) DEM maps under severe illumination differences. Taken together, these planetary mapping studies demonstrate that robust bundle adjustment is indispensable for planetary mapping.

2.4 Remaining Gap

Despite the progress above, a gap still exists between case-specific planetary mapping studies and a reusable quality-control framework for large-scale bundle adjustment. Existing studies usually describe successful workflows for particular sensors or regions, but relatively few works organize the practical experience into a generalized and modular framework that can guide future projects across different data sources. This gap motivates the present study.

3. Quality Control Methods

To make the quality-control procedure more interpretable and executable, we divide the large-scale bundle-adjustment workflow into four interconnected stages: data preprocessing, control-network construction, parameter setting, and post-adjustment accuracy evaluation. This categorization follows the actual processing sequence of large-scale photogrammetric projects. Large-scale planetary bundle adjustment is not an isolated optimization step, but a complete engineering chain that starts from raw images and ancillary SPICE information, passes through four tightly coupled quality control stages, and finally produces refined exterior orientation parameters for reliable DOM and DEM generation. Stage 1 addresses data suitability, Stage 2 addresses the construction of a high-quality network, Stage 3 focuses on error-model selection and bundle-adjustment parameter setting, and Stage 4 verifies the final solution statistically and cartographically.

https://doi.org/10.5194/isprs-archives-XLIX-B3-2026-1223-2026

3.1 Data Preprocessing

The preprocessing stage is the first step of the quality-control chain, because it determines whether the input images are sufficiently consistent and reliable for costly large-scale adjustment. In practical projects, many problems that later appear as network weakness or unstable adjustment behavior can often be traced back to inadequate assessment at the data preprocessing stage. The objective of preprocessing is to evaluate both data suitability and processing risk before control-network construction begins. Metadata analysis including image resolution, incidence angle, emission angle, phase angle, sun azimuth, and acquisition time provides a first-level basis for judgment. These factors jointly affect stereo geometry, radiometric consistency, and the expected success rate of matching. Radiometric inspection is also necessary to identify shadows, weak-texture areas, and severe brightness differences. Because these factors directly influence the robustness of later tie-point extraction.

We strongly suggest that data preprocessing should also include an initial geometric quality evaluation rather than relying only on metadata. A practical strategy is to generate approximate orthophotos from the initial orientation parameters and available terrain data (e.g., LOLA DEM), and then evaluate the relative geometric consistency between adjacent images or the absolute discrepancy with existing mapping products. This approximate-orthophoto based geometric evaluation provides a direct indication of the actual positioning and pointing quality before bundle adjustment. It also helps determine whether certain images should receive lower weights, special handling, or even be excluded from the selected block. Similar ideas have proved effective in large-scale Mars mapping, where initial geopositioning accuracy was quantitatively evaluated before formal adjustment and then used to support later weight design and abnormal-image detection (Geng et al., 2022).

The main issue in this stage is therefore how measurable indicators should be interpreted in relation to downstream tasks and terrain conditions. Although previous studies have reported preferred ranges for solar azimuth, incidence angle, and image observation geometry, practical mapping conditions are often much more complicated. These indicators should therefore be considered jointly with image availability and the adopted mapping methodology, rather than used as rigid thresholds. For this reason, no overly specific criteria are given here. Specifically, in lunar polar regions, the persistently low solar elevation angle and associated illumination conditions often require the image-selection criteria to be relaxed appropriately. Rather than applying overly strict thresholds, it is generally preferable to retain a broader set of mutually complementary images for joint processing, thereby maximizing the usable image extent. Therefore, the output of Stage1 is not only a selected image set, but also a structured prior assessment of image quality and geometric reliability. This output corresponds directly to the items in Table1 and provides the basis for the subsequent design of image overlap relationships, matching strategies, and constraint settings.

From a project-management perspective, this stage also reduces downstream cost and uncertainty. If obviously unsuitable images, highly inconsistent illumination groups, or geometrically abnormal strips are identified early, later control-network construction and bundle adjustment become much more controllable. Conversely, if these issues are ignored in the beginning, they often reappear later as unstable matching, excessive outliers, or even failure to converge. In this sense, data preprocessing is not only technical preparation, but also the stage at which major processing risks are identified and handled.

Items	Main criteria
Metadata analysis	Examine resolution, incidence angle, solar azimuth, emission angle, phase angle, and acquisition time to assess stereo strength, illumination consistency.
Image radiometric quality evaluation	Quantify shadow proportion, weak-texture coverage, local contrast, and severe radiometric inconsistency between overlaps.
Initial geometric accuracy evaluation	Evaluate relative offsets between adjacent images and absolute discrepancies with available controlled basemaps.
Image selection	Select images by balancing overlap completeness, stereo intersection geometry, illumination distribution, and expected matching reliability.

Table 1. Data Preprocessing.

3.2 Control Network Construction

USGS ISIS provides a relatively complete processing chain for control-network generation, including overlap analysis, tie points seed generation, control measures refinement, image matching, and interactive inspection through tools such as *findimageoverlaps*, *autoseed*, *cnetref*, *pointreg*, *qnet*, *cneteditor*, and *cnetstats* (Edmundson et al., 2012). However, for very large planetary image blocks, the availability of these software modules does not automatically guarantee that a control network can be constructed efficiently or robustly. In practice, this stage remains the most time-consuming and operationally sensitive part of the workflow. It is also the stage that most strongly determines the quality of the subsequent bundle adjustment.

The critical objective is not merely to maximize the number of tie points, but to build a network that is spatially balanced, and sufficiently reliable for later adjustment. Here, “spatially balanced” specifically refers to the tie-point distribution within each overlapping stereo pair, rather than to the distribution within an individual image or within a certain surface region. Indeed, this aspect is difficult to evaluate with the assistance of current software tools. The selection of matching pairs should itself be treated as a quality-control decision, because not all overlap pairs contribute equally to downstream stability (Qin, 2019). Overlap analysis defines the feasible topology of the block; matching strategy and tie-point density determine the observation pattern; and external control plus outlier rejection determine whether the network remains stable at scale. In practical projects, network design should therefore be judged from both geometric and graph-structural perspectives. A block may contain many measures overall but still remain weak in critical cross-strip links, boundary areas, or low-texture subregions. Conversely, some tie points that appear redundant from a purely statistical perspective may still be important because they preserve long-distance strip connections or stabilize regions with weak stereo geometry. For this reason, network inspection should pay attention not only to point counts and residual magnitudes, but also to the spatial distribution of reliable links across the full block. Matching methodology is therefore another important source of uncertainty. In practical large-scale Mars and lunar processing, adaptive rather than uniform network design is usually preferable.

We recommend orthophoto-space matching as a practical option for large-scale planetary control-network construction. Approximate DOMs generated from a DEM together with initial position and attitude information provide a geometrically normalized matching domain, reducing the influence of pushbroom distortion, terrain deformation, and part of the viewpoint difference. This strategy has proved effective in both large-scale regional Mars processing and difficult lunar south-polar workflows (Geng et al., 2022, Wang et al., 2025), and it is also supported in the photogrammetric processing chain of NASA ASP. Before formal bundle adjustment begins, gross mismatches should be removed as much as possible. We suggest that the outliers can be detected and removed in orthophoto space using robust estimators such as RANSAC. Because high-precision horizontal control is often unavailable, external reference information is also important. Thus DEM-assisted refinement remains necessary. Because the control network is the direct carrier of image observations in bundle adjustment, quality control in this stage largely determines whether the solution is stable, accurate, and scalable.

In addition, learning-based matching methods can be used to improve the robustness of tie-point extraction, but they still do not remove the need for quality-control procedures. The main issues in this stage are therefore how to design the network topology and tie-point density according to the actual image distribution, terrain conditions, and expected error patterns; how to detect and remove outliers in a timely manner; and how to introduce external control information to stabilize the network. These issues are summarized in Table 2. For large-scale projects, control network optimization is also necessary to reduce computational cost while preserving sufficient spatial coverage and connectivity. Too many redundant points increase the burden of adjustment, whereas too few points may weaken the network or make it unstable. At present, however, effective software tools for large-scale control-network quality assessment and optimization are still lacking.

Items	**Main criteria**
Calculate overlapping relationship	Determine overlap ratio, stereo-pair availability, and network connectivity for the full image block.
Set matching method and tie point density	Choose matching strategy and tie-point pattern according to texture richness, error correction model, and computational cost.
Outlier detection before BA	Remove gross mismatches using geometric consistency in orthophoto space based on robust estimators such as RANSAC.
Add absolute control data	Introduce external height or planimetric constraints through DEM/DOM matching or other geodetic references.
Outlier detection during BA	Iteratively inspect residual distributions, image-wise abnormal measures, and unstable image islands during adjustment.
Control network optimization	Reduce redundant points while preserving spatial coverage, strip connections, and image-wise observation balance.

Table 2. Control Network Construction.

3.3 Parameter Setting During Bundle Adjustment

Once a reliable control network has been established, the next challenge is to transform the image observations into a stable and well-constrained adjustment solution through appropriate error correction model and weight strategies. As summarized in Table 3, the central issue in this stage is not parameter tuning in isolation, but matching the correction model and weights to the actual image error characteristics. Take the bundle-adjustment method implemented in USGS ISIS (i.e., JIGSAW program) as an example, the correction model should be selected according to the expected positioning and pointing error characteristics rather than fixed *a priori* for all datasets (Edmundson et al., 2012). For some datasets, a constant correction term may be sufficient, whereas other datasets may require linear drift terms or higher-order correction components to compensate for more complex orientation errors. The linear and especially quadratic terms place stronger demands on the spatial distribution and geometric strength of tie points. If the control network is unevenly distributed or weakly connected, the additional degrees of freedom may be absorbed in an unstable manner, leading to parameter correlation or physically unreasonable corrections. Therefore, higher-order terms should only be introduced when they are supported by clear error patterns, adequate observation redundancy, and physically reasonable correction magnitudes. To make this model choice more explicit, the residual position and attitude corrections can be represented as quadratic functions of imaging time:

$$\begin{cases} \Delta X_t = X_0 + X_1 t + X_2 t^2, \\ \Delta Y_t = Y_0 + Y_1 t + Y_2 t^2, \\ \Delta Z_t = Z_0 + Z_1 t + Z_2 t^2, \\ \Delta \omega_t = \omega_0 + \omega_1 t + \omega_2 t^2, \\ \Delta \phi_t = \phi_0 + \phi_1 t + \phi_2 t^2, \\ \Delta \kappa_t = \kappa_0 + \kappa_1 t + \kappa_2 t^2. \end{cases} \tag{1}$$

Here, t denotes the image time variable. The terms ΔX_t, ΔY_t, and ΔZ_t describe the time-dependent translational corrections, whereas $\Delta\omega_t$, $\Delta\phi_t$, and $\Delta\kappa_t$ denote the corresponding angular corrections. For each component, the coefficients such as (X_0, X_1, X_2) or $(\omega_0, \omega_1, \omega_2)$ represent the constant, linear, and quadratic terms to be estimated in the adjustment.

Another practical issue is that we usually implicitly assume that the adjusted images can be described, at least approximately, by a common error model. This assumption is often acceptable for a relatively homogeneous block acquired within a limited time span, but it becomes weaker for large-scale planetary datasets involving images collected over long periods or under obvious different illumination conditions. In such cases, forcing all images to follow an overly uniform correction model may hide the actual data heterogeneity. In practical large-block Mars images processing, Geng et al. (Geng et al., 2022) showed that weights can be specified more reasonably when they are linked to the initial geopositioning evaluation of approximate orthophotos, and that abnormal images may require special handling instead of being forced into a single global solution. In weak-convergence lunar polar blocks, DEM-based topographic constraints and external elevation references such as LOLA-related products further provide an effective way to stabilize the adjustment without relying exclusively on tie points (Wu et al., 2014, Chen et al., 2024, Wang et al., 2025). These experiences indicate that model selection, weight setting, and pre-adjustment should be treated as a coupled quality-control process rather than as isolated decisions. Before the formal adjustment is carried out, a strict pre-adjustment step can then be used to identify hidden problems in the control network and parameter settings, and to determine whether additional model flexibility is genuinely improving the solution rather than merely absorbing noise.

The parameter-setting stage transforms empirical knowledge into explicit numerical constraints, thereby bridging the gap between the raw control network and a stable adjustment solution. In bundle adjustment, the weights essentially determine the degree to which the observations are allowed to deviate during the adjustment process. Therefore, the outputs of this stage are not limited to a converged least-squares solution, but include physically interpretable corrections of position and attitude parameters, a rational weight configuration. This interpretation is consistent with the quality-control items listed in Table 3.

Items	Main criteria
Mathematical model	Select error correction terms according to the magnitude and pattern of initial geometric errors, such as constant, drift, or higher-order components.
Weight setting	Define the constraint weights for the expected magnitudes of position corrections, attitude corrections, and ground-point corrections. These weights are derived from initial geopositioning quality, control reliability, matching precision, and prior engineering knowledge.
Pre-adjustment	Perform a preliminary adjustment to expose unstable images, abnormal residual clusters, and incompatible parameter settings before the formal solution.

Table 3. Parameter Setting During Bundle Adjustment.

3.4 Accuracy Evaluation After Bundle Adjustment

Even a numerically convergent solution does not necessarily guarantee a geometrically reliable result. Therefore, a multi-level accuracy-evaluation framework is indispensable after bundle adjustment. As summarized in Table 4, accuracy evaluation should be treated as a layered diagnostic process rather than a single acceptance test. Sigma naught provides only a global fit indicator; local residual patterns, covariance-based point uncertainty, and exterior-orientation corrections reveal whether the solution is locally stable; and forward-intersection errors, strip-to-strip consistency, and agreement with external references determine whether the adjusted block is trustworthy.

More importantly, this stage is the direct bridge from adjustment computation to product generation. The refined exterior orientation parameters are not an end in themselves; their value is ultimately reflected in the quality of the derived DOMs and DEMs. For this reason, post-adjustment evaluation should determine not only whether the least-squares solution has converged, but also whether the updated orientation parameters are reliable enough for downstream mapping products.

A practical evaluation strategy is to begin with low-cost product-level checks before generating full high-resolution products for the entire block. For example, after bundle adjustment, one may first use an available reference DEM to generate approximate or moderate-resolution DOMs and then analyze the geometric consistency of adjacent orthophotos in overlapping areas. If neighboring DOMs still exhibit local offsets, strip discontinuities, or unstable seams, these problems usually indicate remaining issues in tie-point reliability, network geometry, or parameter setting. Likewise, selected sample areas can be used to generate local DEMs or partial stereo products so that terrain continuity and local intersection quality can be examined before the full production workflow is executed.

Items	Main criteria
Sigma naught	Use sigma naught as a global indicator of the bundle adjustment solution.
Residuals of control measures	Inspect residual magnitude, root mean square errors (RMSEs), and spatial clustering for measures, images, and strips.
Theoretical positioning accuracy of tie points	Analyze covariance-propagated point uncertainty to assess internal network strength.
Corrections of the exterior orientation	Check whether position and attitude corrections remain physically reasonable and consistent with prior navigation and pointing quality.
Forward intersection errors	Examine the residual three-dimensional intersection error after adjustment.
Relative geometric accuracy evaluation	Compare adjacent strips or overlapping products derived from refined EO parameters.
Absolute geometric accuracy evaluation	Compare DEM/DOM products with external references to evaluate absolute positioning accuracy.

Table 4. Accuracy Evaluation After Bundle Adjustment.

4. Experimental Results and Discussion

4.1 Experimental Datasets

To demonstrate the effectiveness of the proposed quality-control framework, we conducted experiments using LRO NAC images, and the results are summarized in Table 5. The datasets differ significantly in data volume and processing complexity, thereby providing a practical test of the framework under different conditions. In particular, Dataset 1 is located in the lunar polar region and is characterized by rugged terrain, poor illumination conditions, and repeated overlapping coverage. Dataset 2 covers a much larger area with several thousand images. The photogrammetric processing of both datasets is highly challenging.

4.2 Experimental Results

The experimental results indicate that satisfactory bundle-adjustment solutions can be achieved for both datasets when the proposed framework is applied. The sigma naught values are 0.53 for Dataset 1 and 0.77 for Dataset 2, while the numbers of control points and control measures increase from tens of thousands to millions as the data scale increases. These results suggest that the proposed workflow remains effective not only for medium-scale projects but also for much larger planetary image blocks. Figure 1 and Figure 2 show the image distribution, illumination conditions, and overlap relationships of

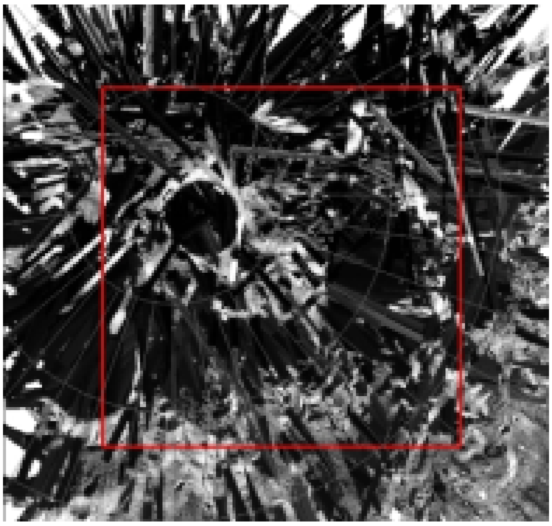

(a)

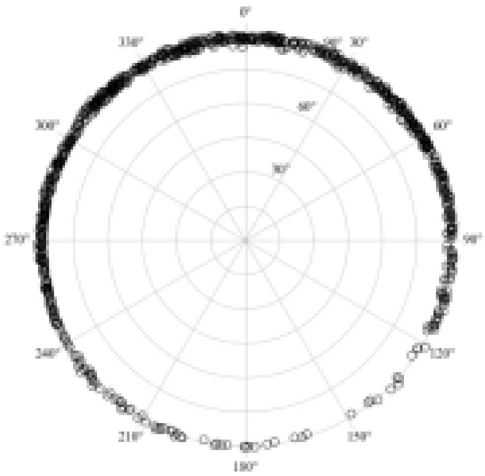

(b)

Figure 1. Image Distribution And Illumination Conditions For Dataset 1: (a) Image Distribution; (b) Sun Incidence Angle And Azimuth Angle.

the experimental datasets. Figure 3 shows the geometric accuracy evaluation results after bundle adjustment. As can be seen, the relative geometric accuracy between adjacent strips is sufficiently high. Matching between the generated DEM and the existing LOLA DEM can be used to evaluate both horizontal and vertical accuracy. The results show that the horizontal displacement between the generated DEM and the LOLA DEM is less than 20 m.

Item	Dataset 1	Dataset 2
Images	791	8482
$Sigma_0$	0.53	0.77
Control points	431960	6009450
Control measures	2037070	22046855

Table 5. Bundle Adjustment Results Of The Experiments Using LRO NAC Images.

Figure 2. Image Overlap For Dataset 2.

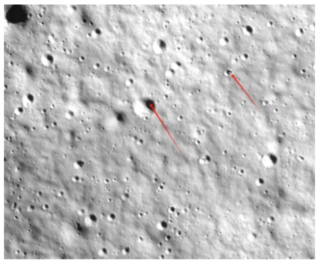

(a)

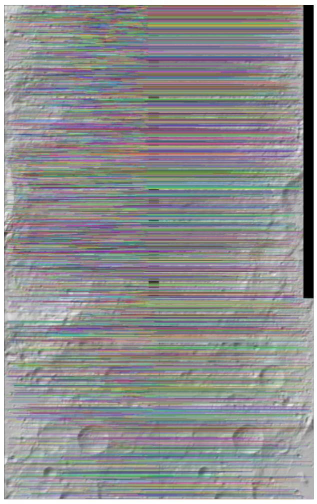

(b)

Figure 3. Geometric Accuracy Evaluation After Bundle Adjustment For Dataset 2: (a) Relative Geometric Accuracy Evaluation For Adjacent Strips; (b) Matching With Existing LOLA DEM For Horizontal And Vertical Accuracy Evaluation.

4.3 Discussion

The experiments also suggest that control-network construction remains the most critical intermediate stage in the bundle adjustment workflow. If the overlap graph is incomplete, tie-point density is poorly designed, or outliers are not removed in time, later parameter tuning cannot fully compensate for those deficiencies. More broadly, the significance of the proposed framework lies in the fact that these items form a closed-loop quality-control system from data selection to final validation. Another implication is that the quality of large-scale planetary bundle adjustment should not be judged by a single statistic alone. Although sigma naught and residual RMSE values are useful for overall diagnosis, representative studies have shown that a satisfactory global solution may still coexist with local weaknesses related to poor tie-point coverage, unstable image islands, or insufficient absolute control. For this reason, residual statistics should be interpreted together with point-distribution analysis, orientation-parameter corrections, and relative or absolute consistency checks on derived DOM and DEM products. Only this combination can ensure that the final result is both numerically stable and cartographically reliable.

5. Conclusions

This paper summarizes a practical quality-control framework for large-scale bundle adjustment of planetary remote sensing images. Instead of focusing on a single processing step, the framework organizes the overall procedure into four interconnected stages, namely data preprocessing, control-network construction, parameter setting, and accuracy evaluation. In future work, the summarized framework can be extended toward more automated and intelligent processing systems, including AI-assisted parameter recommendation, automatic identification of abnormal images, and scalable processing strategies for even larger planetary image archives.

Acknowledgements

This work was supported by the State Key Laboratory of Spatial Datum under grant SKLSD2025-ZZ-13; the National Natural Science Foundation of China under Grant 42241147; and the Space Optoelectronic Measurement and Perception Lab, Beijing Institute of Control Engineering under Grant LabSOMP-2023-07.

References

Beyer, R. A., Alexandrov, O., McMichael, S., 2018. The Ames Stereo Pipeline: NASA's Open Source Software for Deriving and Processing Terrain Data. *Earth and Space Science*, 5(9), 537–548.

Chen, C., Ye, Z., Xu, Y., Liu, D., Huang, R., Zhou, M., Xie, H., Tong, X., 2024. Large-Scale Block Bundle Adjustment of LROC NAC Images for Lunar South Pole Mapping Based on Topographic Constraint. *IEEE Journal of Selected Topics in Applied Earth Observations and Remote Sensing*, 17, 2731–2746.

Di, K., Liu, B., Peng, M., Xin, X., Jia, M., Zuo, W., Ping, J., Wu, B., Oberst, J., 2017. An initiative for construction of new-generation lunar global control network using multi-mission data. *The International Archives of the Photogrammetry, Remote Sensing and Spatial Information Sciences*, XLII-3/W1, 29–34.

Edmundson, K. L., Cook, D. A., Thomas, O. H., Archinal, B. A., Kirk, R. L., 2012. JIGSAW: The ISIS3 bundle adjustment for extraterrestrial photogrammetry. *ISPRS Annals of the Photogrammetry, Remote Sensing and Spatial Information Sciences*, I-4, 203–208.

Fergason, R. L., Lee, E. M., Weller, L., 2013. THEMIS geodetically controlled mosaics of mars. *44th Lunar and Planetary Science Conference*. Abstract #1642.

Geng, X., Xu, Q., Wang, J., Lan, C., Qin, F., Xing, S., 2022. Generation of Large-Scale Orthophoto Mosaics Using MEX HRSC Images for the Candidate Landing Regions of China's First Mars Mission. *IEEE Transactions on Geoscience and Remote Sensing*, 60, 1–19.

Geng, X., Xu, Q., Xing, S. et al., 2020. A Generic Pushbroom Sensor Model for Planetary Photogrammetry. *Earth and Space Science*, 7, e2019EA001014.

Li, C. L. et al., 2018. Lunar Global High-Precision Terrain Reconstruction Based on Chang'e-2 Stereo Images. *Geomatics and Information Science of Wuhan University*, 43(4), 485–495.

Li, D., Yang, B., Wang, M., Wang, T., Gao, Y., Pi, Y., 2023. Large-Scale Automatic Block Adjustment from Satellite to Indoor Photogrammetry. *Geo-spatial Information Science*, 26(2), 160–174.

Liu, P., Geng, X., Li, T., Zhang, J., Ma, X. et al., 2024. The Generation of High-Resolution Mapping Products for the Lunar South Pole Using Photogrammetry and Photoclinometry. *Remote Sensing*, 16(12), 2097.

Pi, Y., Yang, B., Li, X., Wang, M., 2022. Robust Correction of Relative Geometric Errors among Gaofen-7 Regional Stereo Images Based on Posteriori Compensation. *IEEE Journal of Selected Topics in Applied Earth Observations and Remote Sensing*, 15, 3224–3234.

Preusker, F., Stark, A., Oberst, J., Matz, K.-D., Gwinner, K., Roatsch, T., Watters, T. R., 2017. Toward High-Resolution Global Topography of Mercury from MESSENGER Orbital Stereo Imaging: A Prototype Model for the H6 (Kuiper) Quadrangle. *Planetary and Space Science*, 142, 26–37.

Putri, A. R. D., Sidiropoulos, P., Muller, J. P., Walter, S. H. G., Michael, G. G., 2019. A New South Polar Digital Terrain Model of Mars from the High-Resolution Stereo Camera (HRSC) Onboard the ESA Mars Express. *Planetary and Space Science*, 174, 43–55.

Qin, R., 2019. A Critical Analysis of Satellite Stereo Pairs for Digital Surface Model Generation and a Matching Quality Prediction Model. *ISPRS Journal of Photogrammetry and Remote Sensing*, 154, 139–150.

Ren, X. et al., 2019. A Global Adjustment Method for Photogrammetric Processing of Chang'e-2 Stereo Images. *IEEE Transactions on Geoscience and Remote Sensing*, 57, 6832–6843.

Robbins, S. J., Kirchoff, M. R., Hoover, R. H., 2020. Fully Controlled 6 Meters per Pixel Mosaic of Mars's South Polar Region. *Earth and Space Science*, 7, e2019EA001054.

Robbins, S. J., Kirchoff, M. R., Hoover, R. H., 2023. Fully Controlled 6 Meters per Pixel Equatorial Mosaic of Mars from Mars Reconnaissance Orbiter Context Camera Images, Version 1. *Earth and Space Science*, 10, e2022EA002443.

Robinson, M. S., Brylow, S. M., Tschimmel, M., Humm, D., Lawrence, S. J., Thomas, P. C., Denevi, B. W., Bowman-Cisneros, E., Zerr, J., Ravine, M. A., Caplinger, M. A., Ghaemi, F., Schaffner, J. A., Malin, M. C., Mahanti, P., Bartels, A., Anderson, J., Tran, T. N., Eliason, E. M., McEwen, A. S., Turtle, E., Jolliff, B. L., Hiesinger, H., 2010. Lunar Reconnaissance Orbiter Camera (LROC) Instrument Overview. *Space Science Reviews*, 150(1–4), 81–124.

Sidiropoulos, P., Muller, J. P., Watson, G., Michael, G., Walter, S., 2018. Automatic Coregistration and Orthorectification (ACRO) and Subsequent Mosaicing of NASA High-Resolution Imagery over the Mars MC11 Quadrangle, Using HRSC as a Baseline. *Planetary and Space Science*, 151, 33–42.

Wang, S., Geng, X., Li, J., Li, T., Yu, J., Wang, A., Wang, J., Liu, P., Peng, Z., Ma, X., Wang, Y., Wang, Y., Chang, G., 2025. Control Network Construction for LRO NAC Images Based on Refining Tie Points by Matching with Shaded LOLA DEM. *IEEE Journal of Selected Topics in Applied Earth Observations and Remote Sensing*, 18, 25512–25531.

Wu, B., Hu, H., Guo, J., 2014. Integration of Chang’e-2 Imagery and LRO Laser Altimeter Data with a Combined Block Adjustment for Precision Lunar Topographic Modeling. *Earth and Planetary Science Letters*, 391, 1–15.

Yang, B., Wang, M., Xu, W., Li, D., Gong, J., Pi, Y., 2017. Large-Scale BA without Use of Ground Control Points Based on the Compensation of Geometric Calibration for ZY-3 Images. *ISPRS Journal of Photogrammetry and Remote Sensing*, 134, 1–14.